Tutor/s

Dra. Mercè Granados Juan
Departament de Enginyeria Química i Química Analítica

Dra. Alba Lozano Letellier
Institut de Diagnosi Ambiental i Estudis de l'Aigua (CSIC)

Grau de Química

Treball Final de Grau

Study of the phosphorus adsorption capacity of synthetic basaluminite using a fixed-bed column.

Estudi de la capacitat d'adsorció de fòsfor de la basaluminita sintètica utilitzant una columna de llit fix.

Ramon Bargalló Expósito

June 2020

Universitat de Barcelona

B:KC Barcelona Knowledge Campus
Campus d'Excel·lència Internacional

Estic molt agraït a la Dra. Alba Lozano, tutora del CSIC, per tota la seva ajuda, per guiar-me en el desenvolupament del treball durant aquests mesos i per donar-me la oportunitat de veure la manera de treballar en un centre d'investigació. La seva predisposició a resoldre els dubtes i a guiar-me tant en el procés experimental com en el teòric i bibliogràfic, és un fet molt recalcable i que ha facilitat en gran mesura l'execució d'aquest projecte. Pel que fa al CSIC, també vull agrair l'ajuda del tècnic de laboratori Jordi Bellés per la seva ajuda al laboratori, on sempre estava amb un gran somriure.

Pel que fa a la universitat, vull agrair a la meva tutora la Dra. Mercè Granados per la seva ajuda amb tot el tema de format del treball i per ajudar-me en tot el que he necessitat pel que fa a correccions i resolució de dubtes.

Per altra banda, els consells rebuts pels companys i amics, tant de dins del grau, com externs sobre com encarar i millorar un treball d'aquestes dimensions, també ha estat una ajuda molt favorable que ha permès acabar l'estudi de forma satisfactòria. Esmentar especialment a en Joan Marqués, que ha estat company meu en el laboratori del CSIC, ja que teníem projectes molt similars, i ha sigut de gran ajuda.

Per últim, agrair a tota la meva família el seu suport incondicional, el suport donat al llarg d'aquest període m'ha servit com a catalitzador per donar-me impuls moral quan els ànims minvaven.

REPORT

CONTENTS

1. SUMMARY

During the last decades, the phosphorus concentration in wastewaters has increased worldwide causing water eutrophication. Thus, many studies have focused on looking for conventional and non-conventional methods and materials for phosphorus removal. One of the non-conventional materials is the acid mine drainage sludge which has been previously studied as phosphorus adsorbent with good results. This fact motivates the study of basaluminite, an aluminum oxy-hydroxysulfate, one of the compounds of the sludge that can precipitate separated from the rest of acid mine drainage sludge, and which is expected to be a good phosphorus adsorbent.

A fixed-bed column using synthetic basaluminite has been constructed to know the P sorption capacity in this mineral. First, a tracer test has been carried out to determine the porosity and the average residence time of the column with a result of 0.34 and 31.20 minutes, respectively. After that, a breakthrough curve has performed measuring daily the phosphorus concentration from column effluent daily in order to calculate the adsorption phosphorus capacity in basaluminite. These results conclude that synthetic basaluminite presented a maximum phosphorus adsorption capacity of 46.0 mg P/g adsorbent. It has a similar adsorption capacity than schwertmannite and natural basaluminite and, a better capacity than other sorbents such as activated aluminum oxide or magnetic iron oxide. As a conclusion, the basaluminite, a non-conventional material which was a residue at first, has proved to be a remarkable P adsorbent compared to other commercial adsorbents.

Keywords: Phosphorus removal, adsorption capacity, synthetic basaluminite, acid mine drainage, breakthrough curve, tracer test.

2. RESUM

Durant les últimes dècades, la concentració de fòsfor a les aigües residuals ha augmentat arreu, provocant la seva eutrofització. Per tant, molts estudis s'han centrat en trobar mètodes i materials convencionals i no convencionals per a l'eliminació de fòsfor. El fang de drenatge àcid de mina, un material no convencional, s'ha estudiat prèviament com adsorbent de fòsfor amb bons resultats. Aquest fet motiva l'estudi de la basaluminita, un hidroxisulfat d'alumini del que s'espera que serà un bon adsorbent de fòsfor i que pot precipitar independentment de la resta del fang de drenatge àcid de mina,.

En aquest treball es descriu i es porta a terme la construcció d'una columna de llit fix amb basaluminita sintètica per tal d'estudiar la capacitat d'adsorció de fòsfor d'aquest mineral. Primerament, es fa un test de traçadors per determinar la porositat i el temps de residència mig de la columna amb uns resultats de 0,34 i 31,20 minuts, respectivament. Després d'això, es realitza una corba de ruptura mesurant diàriament la concentració de fòsfor de l'efluent de la columna amb l'objectiu de calcular la capacitat d'adsorció de fòsfor de la basaluminita. Els resultats conclouen que la basaluminita sintètica, amb un valor màxim de capacitat d'adsorció de fòsfor de 46,0 mg P/g adsorbent, té una capacitat d'adsorció similar a la schwertmannita i la basaluminita natural i també, una millor capacitat que altres sorbents com l'òxid d'alumini activat o l'òxid de ferro magnètic. Com a conclusió, la basaluminita, un material no convencional que era en primer lloc un residu, ha demostrat ser un remarcable adsorbent comparat front altres adsorbents comercials.

Paraules clau: Eliminació del fòsfor, capacitat d'adsorció, basaluminita sintètica, drenatge àcid de mina, corba de ruptura, test de traçadors.

3. INTRODUCTION

3.1. PHOSPHORUS, SOURCES AND APPLICATIONS

Phosphorus (P) is one of the most abundant elements in the Earth. This element is a non-metal and it has an electron configuration ([Ne] $3s^3$ $3p^3$). When P is bounded with oxygen atoms to form phosphate, one electron in the p and in the s orbitals can jump to the d orbital giving the reactivity to the phosphate which has a versatility to react with other compounds, for example, at a cellular level. Thus, this element is essential for life.[1]

The P sources are very diverse among the surface of the Earth. P can be found in minerals, in rocks, such as basaltic weathered rocks, dissolved in water or in organisms. P contained in rocks could be transformed into fertilizers and feeds for aquaculture or farms.[1][2] Also, P exists in natural waters which has different physical compartments such as in colloids, in fulvic and humic acids, or in aquatic organisms among others.[3]

There are more than 100000 known P compounds that can be separated into two groups: inorganic and organic compounds. The first group is composed of orthophosphates, which have discrete PO_4^{3-} ions, and condensed phosphates.[4] Orthophosphates have three possible ion forms which depend on the pH (PO_4^{3-}, HPO_4^{2-}, $H_2PO_4^-$). These P anions can be bounded with calcium cation and form apatites $Ca_5(PO_4)_3X$. Depending on what anion is X, different orthophosphate minerals can be formed, such as chlorapatite (X=Cl), fluorapatite (X=F) or hydroxylapatite (X=OH) which builds animal bones and teeth. Orthophosphate minerals are used in agriculture activities. Other salts can be formed by the previous P anions such as ammonium and calcium phosphates which have applications as fertilizers.[1]

Condensed phosphates (metaphosphates and polyphosphates) are the result of the condensation of two or more orthophosphates anions making tetrahedral chains (polymerization). Metaphosphates are cyclic anions with a $(PO_3)_n^{n-}$ composition and polyphosphates are linear. Condensed phosphates have many applications such as Pb removal

treatments, detergency, water softening, descaling pipes and boilers, food technology, make toothpaste and preventing corrosion, among others.[5]

The second group is the organophosphates, which are formed with P and carbon chain. Organic P compounds are an important part of the total dissolved P compounds in waters. Also, phosphates are important compounds because they are a component of ATP and DNA. There are more applications of organic P compounds like for manufacturing medicines, biomaterials catalysts, compound, batteries among others. But these organophosphates may have a negative impact because they can be employed as nerve agents or pesticides. Besides, P is a persistent pollutant and the excessive loading of P causes the eutrophication of freshwaters.[3][6]

3.2. EUTROPHICATION AND ITS CONSEQUENCES

The global phosphorus cycle is in a constant change because of human activity, such as the exploitation of phosphorus mineral extraction, production by farming practices or the use in detergents and fertilizers. Therefore, the phosphorus fluxes have doubled, which is considered a potential hazard for the ecosystems.[1] The elevated concentration of P in superficial and wastewaters causes freshwaters contamination. Phosphorus is essential for photosynthetic water microorganisms, but if there is an excess of P in waters, an overgrowth of the phytoplankton and marine microalgae can occur. After their death, the plants rot, consuming oxygen. That oxygen decreases in the water, affects the marine ecosystems due to a macro aquatic life decrease. Other animals such as mammals or birds are also affected by the bacteria produced in the waters. This process is known eutrophication and it has become a widespread environmental problem with health and economic consequences. Eutrophication in the USA, for example, is costing over $2\cdot10^{12}$ by year.[2][3]

In Europe, 53% of lakes and dams are eutrophicated. In the rest of the continents, the percentage is similar (except in Africa that is 28%). More than half of the P comes from water treatment plants. The principal sources of P in wastewaters are the human excretion and the use of detergents. For this reason, new laws for decreasing the phosphorus levels in the industrials and municipal residual waters have been created.[7] For example, the U.S.EPA has

established maximum contaminant levels so that the phosphorus level is <20 ppm in the summer station.[8]

Moreover, in Spain, according to the Royal Decree 509 of 15 March 1996, of development of the Royal Decree 11 of 28 December 1995, which the regulations applicable to urban wastewater treatment are established, the determined P limit for the treatment plants effluents of urban wastewaters is 2 ppm P for sensitive or eutrophicated water areas between 10000 and 100000 acres and 1 ppm P for water areas more extensive than 100000 acres (published in Spanish Official State Gazette (BOE)).[9]

Nowadays, the solution is to decrease more the P levels, which are between 5 and 20 ppm in urban residual waters. There are treatments in wastewater plants that decrease the P level from 8-15 ppm to 6-11 ppm. In Europe, for example, the P levels in residual and superficial waters are decreasing between 30-60% since the 1980's. [10]

3.3. TREATMENTS TO ELIMINATE PHOSPHORUS

Wastewater treatment is a process to reduce or eliminate the water pollutants, such as P. This process has 4 stages: pretreatment, primary treatment with the primary sedimentation of biologic precipitates, secondary treatment with activated sludge and tertiary treatment wherein P removal occurs. The conventional treatments are the most used techniques to eliminate P in wastewaters which can be carried out by two forms: biologic via with microorganisms or by precipitation with coagulants (Fe and Al salts or Ca^{2+}). [1]

The process with calcium ions:

Calcium ions are included in the process with $Ca(OH)_2$. This hydroxide reacts with the alkaline wastewater and forms $CaCO_3$ (1). The rest calcium ions react with phosphate to form hydroxyapatite (2). Finally, the waters end with high alkalinity which can be decreased adding CO_2 to continue with the following step. [11]

$$Ca^{2+}_{(aq)} + 2\ HCO^{3-}_{(aq)} + Ca(OH)_{2\,(aq)} \leftrightarrow\ 2\ CaCO_3 \downarrow + 2\ H_2O_{(l)} \quad (1)$$

$$5\ Ca^{2+}_{(aq)} + 3\ PO_4^{3-}{}_{(aq)} + OH^-_{(aq)} \leftrightarrow Ca_5(PO_4)_3(OH) \downarrow \quad (2)$$

The process with iron (Fe) and aluminum (Al) salts:

On the one hand, the aluminum sulfate is usually used to precipitate the aluminum phosphates (Eq. 3). With concentrations between 50 and 200 ppm of aluminum salts, 80-90% of

the phosphorus can be eliminated. On the other hand, the iron sulfate is also employed to reduce phosphorus concentration, with reactions like that described for Al in Equation 3. Sometimes, $Ca(OH)_2$ is added to increase the pH and to facilitate the reaction. [11]

$$Al^{3+}_{(aq)} + H_nPO_4^{3-n}{}_{(aq)} \leftrightarrow AlPO_4\downarrow + nH^+_{(aq)} \quad (3)$$

The two precipitation treatments have three types of processes that depend on the treatment stage where the salts (coagulants) are added, as shown in Figure 1. Firstly, the reagents can be included in the residual waters before the primary sedimentation. In this treatment, the P is eliminated with a 90% efficiency and concentrations lower than 0.5 ppm may be achieved. Secondly, the salts can be introduced in the primary sedimentation effluent. This process is achieved the highest phosphorus elimination efficiency (95%). With this type of precipitation treatment, the final phosphorus concentration is 0.5 ppm and is reached a purer product than the previous type process. However, this treatment has disadvantages like an elevated cost for the large precipitation tanks and sometimes, a diluted effluent. Finally, the salts can be also included in the secondary sedimentation effluent. This treatment is useful for the wastewater plants which are working with activated sludge. For this process, smaller precipitation tanks are necessary and thus, the costs are lower than the previous. However, in this treatment, the P removal efficiency is the lowest (less than 85%).[1][11]

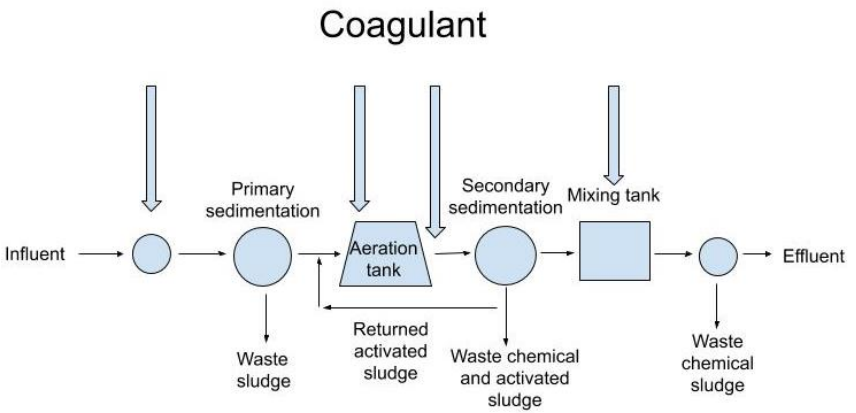

Figure 1. Scheme which indicates where the coagulant can be added depending on the precipitation process. [11]

According to the second conventional method, microorganisms are employed to make aerobic or anaerobic function to remove P. The advantages of this treatment are the cost reduction and the lower sludge production compared to that the precipitation process creates. The P of residual waters is incorporated into the biomass cell which is eliminated into the process as a result of the sludge deposition. The P is accumulated preferably on the bacteria PAO (Phosphorus Accumulator's Organisms) with advantage over other bacteria. The reactor has an anaerobic tank and an activated sludge tank. At first, the PAO organisms accumulate polyphosphates that give energy. With this energy, they assimilate the acetate which is formed through the organic material fermentation. Hence, the PAO produce polyhydroxybutyrate (PHB) and the polyphosphates decrease. Also, orthophosphates, magnesium, iron, potassium and calcium ions are liberated. In the aerobic zone, the storage products are oxidized and the PHB is metabolized. Because of that, energy is produced and is used to form polyphosphate bounds in the cells. However, the orthophosphates are eliminated from the solution and are incorporated into the polyphosphates. Because of these previous processes, the cells grow and when this new biomass with polyphosphates is eliminated, the accumulated P is also eliminated by the bioreactor. [11]

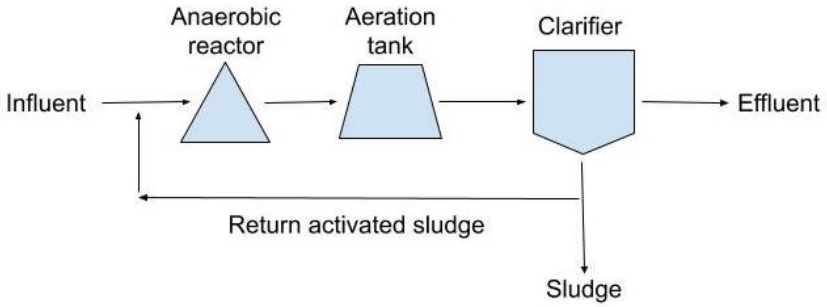

Figure 2. Scheme of the bioprocess to eliminate phosphorus into the bioreactor. [22]

For several years, the objective has been to improve the treatments achieving better P adsorptions on a large-scale. To do that, non-conventional processes with P adsorption in a fixed-bed column were studied. These treatments use different materials which can be gels, ion-exchange resins, bauxite extraction residues, manufactured aluminum or iron oxides and residues of the acid mine drainage, among others.[1] Al and Fe oxides have been used as

phosphate adsorbents with better results than conventional treatments in column experiments, but P adsorption has not used on a large-scale yet. In a laboratory scale, Genz et al. (2004) an effluent concentration of 50 ppb P was reached after a throughput of 4000 bed volumes for activated Al oxide. [12]

Kofinas and Kioussis (2003) studied one of the non-conventional treatment materials to remove P from aquaculture. They used a polymeric hydrogel, achieving more than 98% phosphate removal, decreasing from 16 ppm PO_4^{3-} to 1 ppm PO_4^{3-} after 120 minutes. Hydrogel binds selectively P into the polymeric matrix. Besides, this material can be easily regenerated. Moreover, ion-exchange resins were studied by Zarrabi et al. (2014) with 94.5, 96.3 and 98.7 % of P removal for 20, 30 and 40 mg/L P, respectively, after 150 minutes. Ion-exchange resins had good efficiency at short-time, but P removal efficiency was decreasing as time went by. Liu et al. (2008) with a synthesized mesoporous ZrO_2 resin only removed 58% of phosphorus after one day. These findings demonstrate that these treatments work well on a laboratory scale and at short-time.[13][14][15]

3.4. ACID MINE DRAINAGE

Acid sulfate waters are formed by the sulfide minerals oxidation like the pyrite (FeS_2) (Eqs. (4)(5)(6)). Human activities, such as mining, enhance this spontaneous process due to the major exposure of the minerals to water and air. Thus, groundwater contains a considerable amount of dissolved iron, aluminum and sulfate.[16] The oxidation also causes proton formation which gives the acidity to water. However, this acidity is neutralized by the carbonate rocks, like a buffer. The problem comes when the carbonate rocks presence is not enough, and acid production is higher than the neutralization. Besides, toxic elements like arsenic or uranium are transported too and thus, Acid Mine Drainage (AMD) contaminates lakes or rivers, and the biodiversity is affected.[17]

$$2\ FeS_{2\,(aq)} + 2\ H_2O_{(l)} + 7\ O_{2\,(g)} \leftrightarrow 2\ Fe^{2+}_{(aq)} + 4\ SO_4^{2-}{}_{(aq)} + 4\ H^+_{(aq)} \quad (4)$$

$$4\ Fe^{2+}_{(aq)} + 4\ H^+_{(aq)} + O_{2\,(g)} \leftrightarrow 4\ Fe^{3+}_{(aq)} + 2\ H_2O_{(l)} \quad (5)$$

$$FeS_{2\,(s)} + 14\ Fe^{3+}_{(aq)} + 8\ H_2O_{(l)} \leftrightarrow 15\ Fe^{2+}_{(aq)} + 2\ SO_4^{2-}{}_{(aq)} + 16\ H^+_{(aq)} \quad (6)$$

AMD is one of the earth pollutions responsible for decreasing water quality in rivers, streams or groundwater. It has become a worldwide and long-lived environmental problem and thus, it needs a long-term solution. AMD frequently appears in abandoned mines and the passive treatments (a kind of AMD treatment) can be used in this case to neutralize the acidity. The passive processes may be built with a permeable and reactive substrate to better react with AMD. Some of these acid mine drainage treatments are compost or anaerobic wetlands, which are the most used and have low operational maintenance. This system uses a limestone layer with compost. Also, the precipitation, oxidation and water hydrolysis of the iron and aluminum hydroxides occur in other treatments. Conventional aerobic wetlands are used to remove the water pollutants. The Anoxic Limestone Drain (ALD) is also used, a process that consists on alkalinizing the acid waters with calcite and limestone bed. This system is used to AMD's with very low Fe and Al salts concentrations. ALD is not used for high concentrations because the limestone reacts with Fe and decreases the dissolution rate of the limestone bed. Also, ALD could fail when Al obstructs the pore spaces between limestone rocks (clogging) losing reactivity.[18]

Compost wetlands can solve the clogging issues. Thus, the water is forced to flow down through the layers of limestone and compost. This new treatment is Reducing and Alkalinity-Producing System (RAPS). RAPS mixes compost wetlands and ALD systems. The purpose of the compost layer of this system is to eliminate the oxygen in the water. This causes the reduction of the iron and the limestone layer cannot react with them. However, Al cannot clog the RAPS limestone as the ALD. RAPS are used in AMD's with high pollution. It is also more efficient than the ALD for waters with high Fe and Al salts concentrations. But even then, RAPS can be passivated (loss of reactivity by coating). [18][19]

To solve the loss of reactivity against waters with high metal concentrations and/or high acidity loads, Disperse Alkaline Substrate (DAS) was developed. DAS is composed of alkaline reagent as calcite sand and coarse inert matrix as wood chips. Limestone sand has small size grains that are dissolved before the coating and thus, this composition gives a high reactive surface and high porosity to solve the clogging and passivation problems. Moreover, DAS achieves a high acidity removal by the metal accumulation (Al, Fe, among others). Therefore, DAS has more reactivity than the other explained passive systems and removes the acidity of

AMD four times more efficiently than the other passive treatments on a laboratory scale. Thus, this treatment has been implemented on a larger scale in affected zones by AMD.[20]

Specifically, the Iberian Pyrite Belt (IPB) is a zone in the Southwest of Spain where around 100 abandoned mines drain acid waters, affecting the Odiel and Tinto watersheds, two of the most important rivers in Huelva region. In order to minimize the environmental impact, RAPS and ALD systems were applied, but poor results were achieved because high polluted AMD is a problem for these treatments. Nowadays, DAS is used with a pool with $CaCO_3$ and a limestone bed with a good performance. The AMD is canalized to the pool and then, the calcium carbonate dissolves and wastewater pH increases. The reaction causes sequential precipitation of schwertmannite ($Fe_8O_8(SO_4)(OH)_6$) (3), basaluminite ($Al_4(SO_4)(OH)_{10}\cdot 4H_2O$) (2) and calcite-gypsum (1), as shown the Figure 3. [21] The iron salt is formed first because it needs lower pH than the aluminum salt, which precipitates at approximately pH=4,5.[22] The first aluminum hydrolysis constant is 5.0. When the pH of acid aluminosulphate waters is less than that constant, the equilibrium is controlled by geochemical reactions. However, when the pH is higher, the aluminum salt precipitates.[17][18]

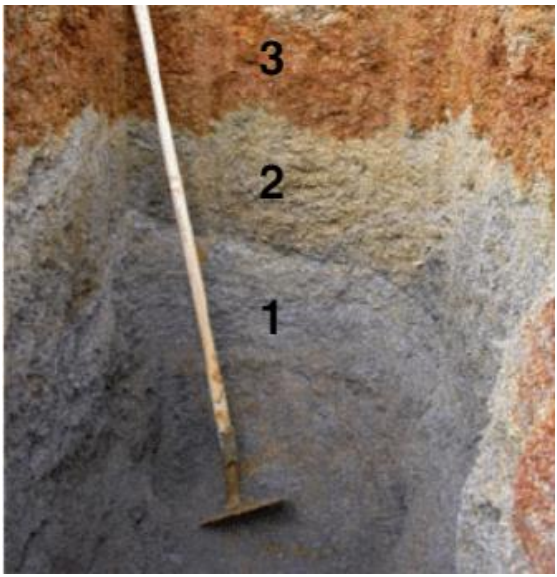

Figure 3. Stratification of the treatment product into the pool. [18]

3.5. BASALUMINITE

A white/yellow mineral was discovered forming 5 mm diameter crystals in an oxidation zone in Felsőbánya, Hungary (nowadays Baia Sprie, Romania). This mineral was named as Felsőbányaite for the locality. Subsequently, Kenngott (1853) was the first scientist who studied this salt. Haidinger (1854) was gave the first description and the molecular formula $Al_4(SO_4)(OH)_{10}{\cdot}4H_2O$ with the help of K. v. Hauer, who performed chemical analysis. On the other hand, Bannister and Hollingworth (1948) identified and described basaluminite and hydrobasaluminite for the first time in Northampton Ironstone (UK). They described these aluminum salts as a white plastic claylike mineral with water. In 1969, Brydon and Singh observed that when basaluminite was with clay minerals, it was precipitated with a more crystalline structure. Hence, the salt structure was a clay and basaluminite mixture. Many years later, Clayton (1980) made a study of them with chemical analysis, XRD data, among other studies. He described the basaluminite unit cell parameters and its structure such as octahedral Al layers with sulfate ions in the interlayer space. Later years, Weiszburg and Papp (1990) established that felsőbányaite and basaluminite could be the same minerals. Farkas and Pertlik (1997) with the structural data and crystal structure determination of the two minerals, established that they were the same because they had the same composition, structure, physical properties and morphology. They also determined the basaluminite structure: eight crystallographically different Al atoms surrounded by oxygens forming AlO_8 distorted octahedral similar to $Al(OH)_3$ structure polymorphs. These octahedrals were making Al_8O_{22} layers that are interconnected between themselves with hydrogen bridges by SO_4 and H_2O molecules as is shown in Figure 4. Moreover, Adams and Rawajfih (1997) described basaluminite as non-crystalline material. Also, the International Mineralogical Association (IMA) does not consider the basaluminite as a mineral. [23][24][25][26][27][28][29][30][31]

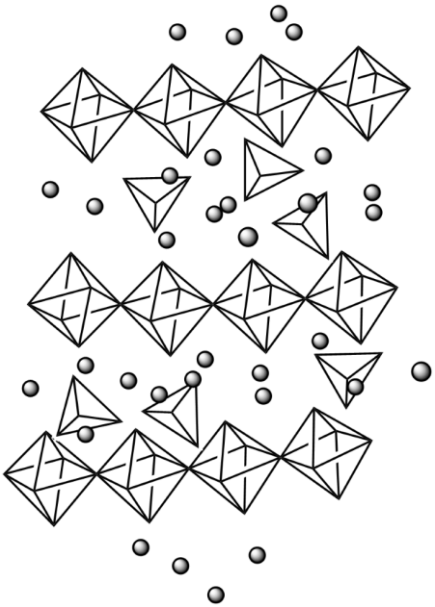

Figure 4. Nanocrystalline basaluminite structure with AlO_6 octahedral forming Al_8O_{22} layers, SO_4 tetrahedra and H_2O molecules shown as single balls made by ChemDraw. [29]

3.6. STATE OF THE ART

The non-conventional treatment to remove the P wastewaters used in this study is the P adsorption with residues of acid mine drainage. The motivation to use this treatment is those good results of P adsorptions registered in previous studies. Sibrell et al. (2008) applied the AMD sludge with results of P adsorption capacities of 20000 mg P/kg sludge at a solution concentration of 1 ppm P. Moreover, at the long-term, process with simulate wastewater with 0,13 ppm P, the AMD sludge removed 60% of P. Also, other long-term tests demonstrated that the sludge can remove 76% of P. Furthermore, the advantages of non-conventional treatments are the non-implantation of larger tanks, which are necessary for conventional treatments, and the simplicity of operation which reduces costs. However, the long-term sustainability of the new technology used in non-conventional treatments has not been demonstrated yet.[32][33]

Technically, adsorption is accumulation of compound (adsorbate) on an adsorbent surface. Adsorption mechanism depends on the surface capacity which is based on the available surface

sites. These adsorption sites limit compound options to accumulate in the adsorbent. The adsorption process could be also based on ion exchange where one ion displaces another one with a lower affinity for the adsorbent. Violante et al. (1996) studied phosphate and oxalate adsorption with Al hydroxysulphate complex. They could not determine the exact mechanisms between the sulfate removal and the other ions sorption. But Genz et al. (2004) determined in their P removal study using activated alumina that the adsorption could be produced by direct competition of anions. Concretely, phosphate and sulfate compete for the activated alumina sites.[34][12]

In wastewaters, the P form is the orthophosphate ion which can be exchanged by the sulfate ion of the Al compound. For the practical part of this study, the adsorbent has been synthetic basaluminite. At first, the phosphorus (phosphates) must access to into the basaluminite interlayer spaces in the adsorption process. These interlayer spaces are occupied by the sulfates (Figure 3), hence there is a competition between the sulfates and phosphates to fill them. According to Rietra et al. (1999), in this competition, the best adsorption is expected for phosphates. [35][12]

Aluminum hydroxysulphate and AMD sludge studies, previously commented, have remarkable P adsorption results. Therefore, basaluminite could be a good P adsorbent. But the difference between other non-conventional treatments is that basaluminite is not a manufactured material, because it is a residue formed by acid conditions. Also, the studies with AMD sludge suggest that it can have a good P adsorption at large-time. Therefore, basaluminite might potentially have a better adsorption capacity than conventional treatments at longer contact-time.

But, will the synthetic basaluminite be a good adsorbent as it is expected both in the short and long term? Will the synthetic basaluminite compete with the other P adsorbents? The experiment at the practical part was prepared in order to answer these questions.

4. INITIAL AIM

This year, an exceptional situation has occurred in all over the world. Coronavirus has forced a lockdown, which started in March, and thus the scheduled experimental study was stopped. The initial aim was to compare the phosphorous adsorption capacity of the basaluminite and the aluminum oxide. To reach this purpose, two fixed-bed columns filled with these both adsorbents were made as described in Appendix 2.

Just one day after the experiments started, the Spanish state declared the confinement due to COVID-19 pandemic. Therefore, the investigation laboratories closed preventing the development of the original study. With this situation and without knowing when the normalization would come back, this work was reoriented. Thus, in order to finish the TFG the laboratory provided experimental results of a fixed-bed column filled with synthetic basaluminite in order to calculate its phosphorus sorption capacity and discuss the results with other sorbents.

5. OBJECTIVES

In this research, the main objective is to test the P sorption capacity of synthetic basaluminite, a mineral of AMD sludge. To reach this principal purpose and to carry out the project step by step, some more specific goals have been considered:

- To determine a tracer test which will provide the porosity of the column and the residence time of the pollutant influent. Both parameters are two specific capacities of the column system. Determinate these capacities are important to know how the adsorbent will adsorb and to compare with others.
- To determine a breakthrough curve for the fixed-bed column, which will help to determine the P adsorption capacity of the synthetic basaluminite.
- To compare the calculated sorption capacity in synthetic basaluminite with that considered in other potential commercial adsorbents.

6. EXPERIMENTAL SECTION

6.1. SYNTHESIS OF SYNTHETIC BASALUMINITE

The fixed-bed column adsorbent was basaluminite synthesized by a drop-by-drop addition of 214 mL 0.015 M $Ca(OH)_2$ to 30 mL 0.05 M $Al_2(SO_4)3{\cdot}18H_2O$ using the EE-1000R (100 µL-1000 µL) electronic pipette. The mix of these commercial reagents was stirred at room temperature until reach a 2.14 OH:Al molar ratio. Basaluminite was precipitated with $CaSO_4{\cdot}2H_2O$. The co-precipitated solid was removed washing three times the Al salt. Finally, the product was dried 48 h at 40ºC with the Memmert oven 100-800. [36]

6.2. MATERIALS AND METHODS

6.2.1. Column setup

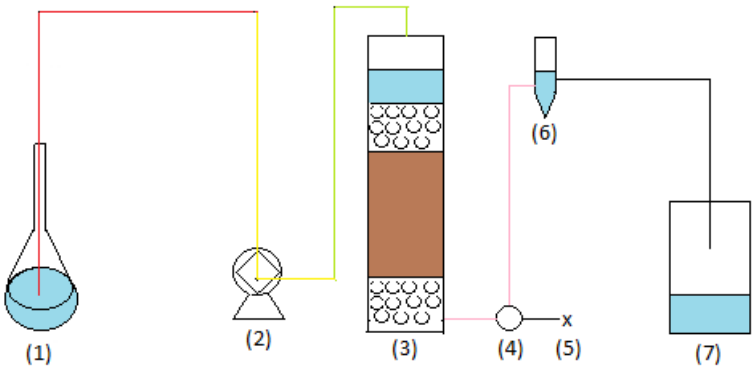

Figure 5. Experimental assemblage design which shows the used instruments interconnected with tubes.

The experimental design is composed of various instruments interconnected as shown in the Figure 5. The volumetric flask (1) contains the solution which will pass through the column. Gilson Minipuls-3 Peristaltic Pump (2) is the instrument that applies the correct solution flow. There is a fixed-bed column (3) which is constructed with a methacrylate tube with 4.20 cm diameter and 0.50 cm thickness. The pink tube relates to the column using a three-way valve (4) which is employed to collect samples (5) for the P analysis. The solution passes through the column from top to bottom and connects to the Schlumberger CTD Diver (6) which collects sample data. After the solution passes through the diver, it ends into a residual flask (7).

Table 1. The tubes measures of the experimental assemblage.

Dimension	Red tube	Yellow tube	Green tube	Pink tube
Longitude (cm)	90	40	70	60
Diameter (mm)	0.80	3.17	0.80	0.80

Fixed-bed column was filled with wood chips (inert matrix) and synthetic basaluminite, as granular adsorbent, like the setup column of a DAS system but only with basaluminite. The aim is to simulate the end of a passive treatment, where the limestone has been dissolved and the basaluminite with the wood chips are filling the gaps.[20]

Hence, 5 g of synthetic basaluminite were weighed on an analytical balance. Then, the salt was mixed in a beaker with the pine chips previously sieved for giving the same chip size and washed to eliminate some organic matter. There was 30 g of the wood chip because 1:6 ratio between the aluminum salt and the wood is desired. This rate was chosen to perform these experiments because it was desired not to lengthen the operation time too much.

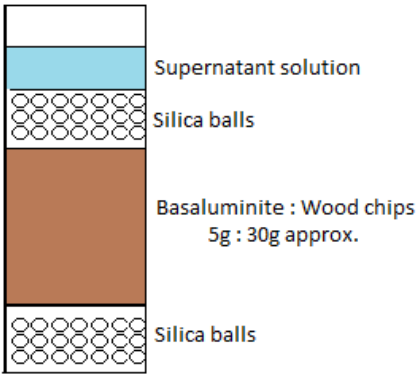

Figure 6. Experimental fixed-bed column scheme that shows the different used compounds.

Firstly, two centimeters of silica pearls were added in the column. Secondly, the mixture of basaluminite and wood was added to the column, ensuring the mixture was compacted making pressure with hands. The column had 12 centimeters of reagent and with the silica pearls, 13.50 cm altogether. The function of these silica balls was to homogenize the superior surface of the mixture and avoid preferred fluxes. Then, the column was saturated with MilliQ® ultrapure water adding 3 cm plus (supernatant) to the total height as shown the Figures 6 and 7. Thus, the total height of the column is 16.50 cm.

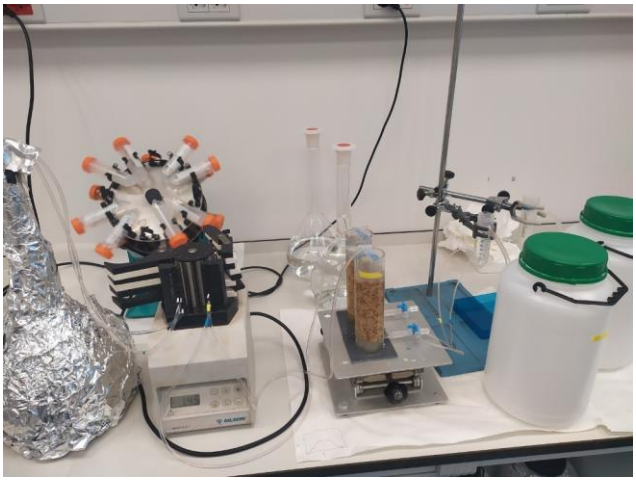

Figure 7. Experimental assemblage in the laboratory wherein only one column and one driver were used for this study.

6.2.2. Tracer test

The tracer test provides the porosity of the column, which is the ratio of pore volume and total volume of the column, and the average residence time of the solution, which is the meantime that the P solution pass through the column. The porosity and the average residence time are two specific attributes of the column which help to describe it.

With the volumetric inflow, the volume of liquid inside the column can be known and with this, the porosity can be calculated. The porosity is a parameter of the column which depends on how much the mineral is compacted. A column with lower compaction has more pores and thus, a bigger porosity than another column more compacted. With the porosity value and the pore volume, the average residence time is calculated.

The experimental determination of porosity and residence time is carried out experimentally by means of techniques where the system is disturbed at the input with a tracer. This causes a response at the output which is function of the mode of flow through the column. A tracer, NaCl solution, is injected into the input current, while the response is the representation of the tracer conductivity in the output current versus time. There is not adsorption of the NaCl by basaluminite because the tracer is a compound that does not react with the adsorbent. The

type of stimulus to be studied is the step type which is the introduction of a constant tracer flow rate into the fluid stream.

To carry out the tracer test 2L of NaCl (sodium chloride 99% ACS REAGENT, SIGMA ALDRICH) solution 0.013M was prepared. Thus, 2.09 g of NaCl was weighed and after that the solid was added with MilliQ® ultrapure water in a 2L flask. This tracer solution had 2 mS/cm conductivity which was measured with the Thermo-scientific Orion Dual Star pH-meter and subsequently, was added to the column by the Gilson Minipuls-3 Peristaltic Pump with a flow of 2.5 mL/min. Throughout the experiment, the CDT Diver Schlumberger was measuring the solution conductivity (mS/cm) of outflow at the bottom of the column every minute. The device is immersed in a 50 mL flask with water and it is employed to regulate the liquid level in the column placing both vessels on the same level. When the solution level of the column increase, the water level in the diver flask decreases until the levels are balanced. With this data, a growth curve of relative conductivity is constructed. Subsequently, 1L of MilliQ® ultrapure water was added to the column to clean it and restore the starting conditions. Similarly, with this data, a decline curve is made to complete the tracer test graph.

6.2.3. Breakthrough curve

A critical aspect of the design of a fixed-bed adsorption column involves the characterization of the effluent concentration profile as a function of the volume processed or the operating time. The dynamic behavior of a fixed-bed adsorption column can be visualized in the active mass transfer zone moving through the bed as a function of the displacement produced by the saturation of the adsorbent.[37]

The mass transfer zone is the bed zone where adsorbate is transferred from the fluid to the adsorbent. The breakthrough point is observed when the front of the mass transfer zone appears in the effluent. Moreover, when the effluent and the influent concentrations are equals is called the exhaustion point where the bed is not capable to remove more adsorbate. The breakthrough curve (BTC) shape relies on the properties of the adsorbent and adsorbate, the bed depth and the flow velocity of the process. BTC data of the fixed-bed column is analyzed and used to optimize the performance and operation of the column.[37]

The BTC is used to determine the basaluminite P adsorption capacity. For this study, a H_2PO_4 (potassium phosphate monobasic SIGMA-ALDRICH) solution (1.13 ppm P) was injected to the column using the same flow as the tracer test. Using the three-way valve connected with the column, 5 mL solution samples were collected two times every day using the EE-1000R (100 µL-1000 µL) electronic pipette. Thei P concentrations were measured weekly using the Murphy and Riley method to make a BTC as shown in the Figure 8.

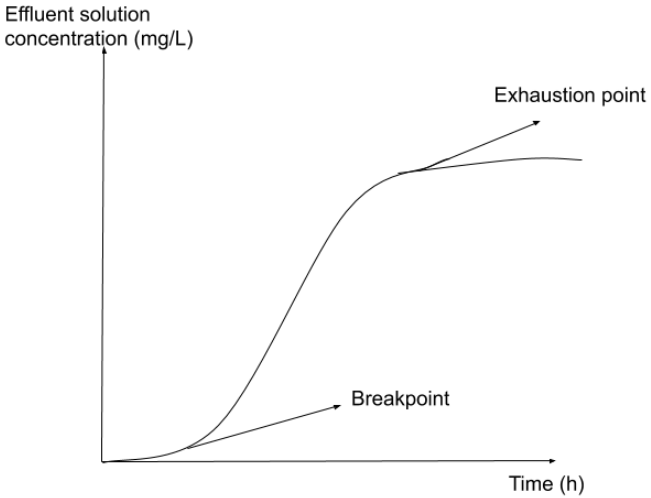

Figure 8. BTC scheme where the breakpoint and the exhaustion point are located.

5.2.4. Murphy and Riley method

Phosphate analyses are dominated by methods which utilize the reaction between the phosphate and molybdate ions. Among them, the most used method for natural waters and employed in this work is described by Murphy and Riley. They used an acidified (with sulfuric acid 95-97% MERCK) solution of ammonium molybdate tetrahydrate SIGMA-ALDRICH with antimony (gives by potassium antimonyl tartratetrihydrate SIGMA-ALDRICH) and ascorbic acid 99% ACROS ORGANICS. This reagent reacts rapidly with the phosphate ion-producing a blue-purple compound (named phosphomolybdenum) with an atomic ratio of 1:1 of antimony and phosphorus. The complex is very stable and follows Beer's law up to 2 µg/mL P concentration. Thus, a calibration curve that relates the P concentration in water and the intensity received by the spectrophotometer is made with P solutions with known

concentrations. Then, this calibration gives the P concentration value of the samples analyzed which are known as Soluble Reactive Phosphorus (SRP), Molybdate Reactive Phosphorus (MRP) or Dissolved Reactive Phosphorus (DRP).[3][38]

This method of analysis consists of a mixture of 10 mL of the sample, which is filtered with a 0.45 µm nylon filter, and 10 mL of the standard solutions with 1 mL of the reagent 1 and 0.2 mL of the reagent 2 recollected using the EE-1000R (100 µL-1000 µL) electronic pipette. The sample solutions are placed in the dark for 45 min. Then, SP-830 Metertech Plus spectrophotometer is calibrated with the blank solution. Finally, standard and sample solutions are analyzed using a wavelength of 880 nm.

Reagent 1: 0.2 g $C_4H_4O_7SbK \cdot 3H_2O_{(s)}$ (antimony potassium tartrate trihydrate SIGMA-ALDRICH) are transferred to a 1L volumetric flask and 500 ml of MilliQ® ultrapure water are added. When the solid is dissolved, 111 mL concentrated $H_2SO_{4\,(l)}$ and 11.2 g $(NH_4)_6Mo_7O_{24} \cdot 4H_2O_{(s)}$ (ammonium molybdate tetrahydrate SIGMA-ALDRICH) are added to the solution which must be cooled because the process is exothermic. When the temperature decreases, the flask is made up to volume with MilliQ® ultrapure water. This reagent should be kept in the refrigerator.

Reagent 2: 27 g $C_6H_8O_{6\,(s)}$ (ascorbic acid 99% ACROS ORGANICS) are dissolved in 500 mL of MilliQ® ultrapure water. This reagent should be kept in the refrigerator with a packaging which does not allow light to pass through because UV light can degrade the reagent.

7. TRACER TEST

Figure 9 shows the conductivity of the outflow which has passed through the column along the time during the tracer test. In this graph, two types of curves can be distinguished: firstly, the growth curve shows the NaCl solution passing through the column (the 50 mL flask where the diver is placed measures the solution conductivity). Secondly, a decreasing curve is displayed after 1 L of MilliQ® ultrapure water is added, and thus the initial conditions are restored (the diver measures the conductivity decrease as the MilliQ® ultrapure water leaves the column). In the growth curve, when the tracer solution has passed through the column after 3h approximately, the tracer measures the maximum conductivity of the NaCl solution. Moreover, in the decline curve, the tracer measures less and less conductivity because the NaCl solution has been replaced by the water in the 50 mL flask. This process has taken 4 h. Bubbles in the column, which were formed where the column was filled for the first time, can cause irregularities in the growth curve. When NaCl solution passes through the column, the bubbles were removed and thus, the decline curve came up with a better form.

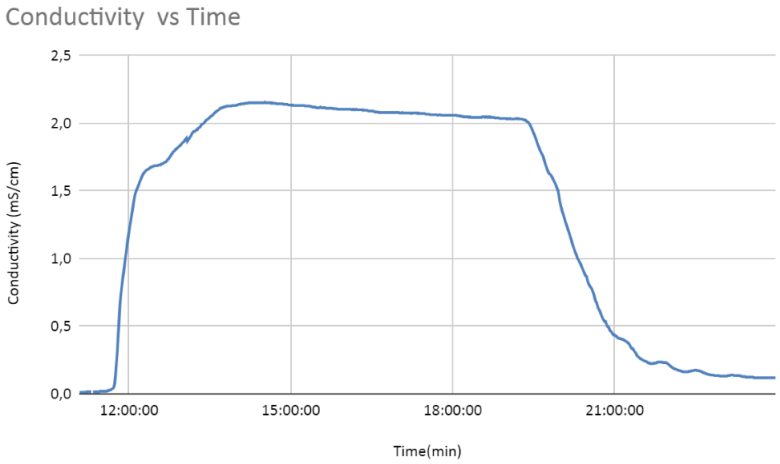

Figure 9. Tracer test graph which represents the conductivity (mS/cm) vs the time (min).

With the equations (7)(8)(9)(10) and (11), the porosity and the average residence time of the column have been determined. To calculate these values, the decline curve of the tracer test is used because is clearer than the growth curve. Specifically, the curve used was created with the division between the conductivity values of the decline curve and the initial conductivity (y-axis) versus the time (x-axis) as shown in Figure 10. A vertical line has been drawn trying to divide the curve symmetrically, where the surface below the curve is equal to the surface above, as shown in Figure 10.

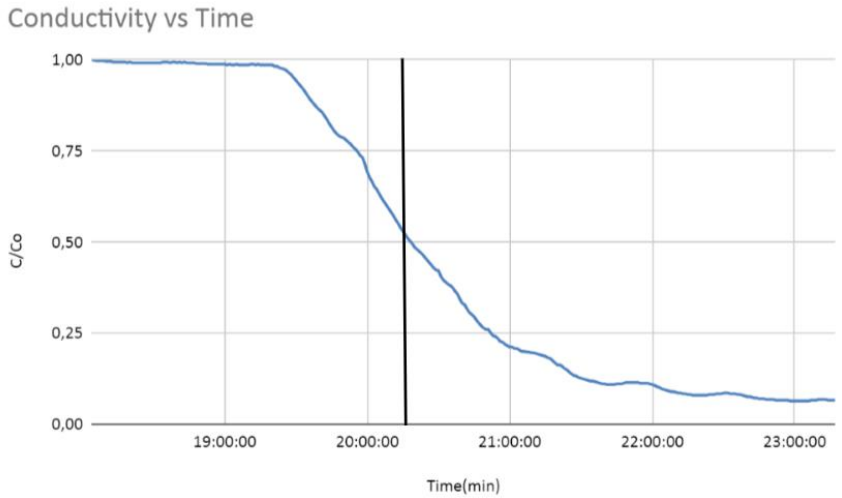

Figure 10. Decline curve graph where the relative conductivity (C/Co) and the mean time (t) are located with the intersection between the line and the curve

$$P = V_{pores}/V_{column} \quad (7)$$

$$V_{pores} = Q \cdot t \cdot C/C_o \quad (8)$$

$$V_{column} = h \cdot a \quad (9)$$

$$A = \pi \cdot r^2 \quad (10)$$

$$R_t = V_{pores}/P \quad (11)$$

Where: V= volume, P= column porosity, Q= input flow, t= mean time, C/C_o= relative conductivity, A= column area, h= column height, r= column radio, R_t= Average residence time.

Table 2. Comparison of the tracer tests results with another basaluminite study [39]

Basaluminite type[(a)]	Relative conductivity	Mean time (min)	Pores volume (cm^3)	Column porosity[(b)]	Average residence time (min)
Synthetic	0.52	60.00	78.00	0.34	31.20
Natural	0.45	115.00	129.38	0.57	51.75

(a) Both studies made the tracer test with a 2.5 mL/min input flow and a 228.60 cm^3 column volume.

(b) The porosity value of a column with spheres bed is considered 0,4. [40]

As Table 2 shows, the column porosity value is 0.34 and the average residence time is 31.2 min for the study with synthetic basaluminite. These values can be compared with Marqués study (2020) which made a tracer test under the same conditions but using a natural basaluminite as adsorbent.[39] The studies with natural and synthetic basaluminite have similar porosity and average residence time results as might be expected because both experiments and adsorbents are practically identical. Though, the column with natural basaluminite has a bit bigger porosity value than the column with synthetic basaluminite because of the compaction of the column reagents. The column with synthetic basaluminite had greater compactness obtaining a lower porosity than the column with natural adsorbent. Moreover, the average residence time of the natural basaluminite column is bigger than the other column because it has more pores volume.

8. BREAKTHROUGH CURVE

As discussed before, basaluminite adsorbs phosphate (P) present in the solution which passes through the column. Aqueous samples at the column outflow were taken for almost four months to study how much P can be retained. Figure 11 shows the P concentration (mg/L) of the samples respect to time (hours). The rise of the curve is relatively slow because P sorption occurs in basaluminite at the beginning of the experiment. The breakthrough point was reached in 52 days and the exhaustion point took a total of 104 days with more than 70% of P adsorbed. There are regions of ups and downs in the curve, which is probably produced by the experimental error.

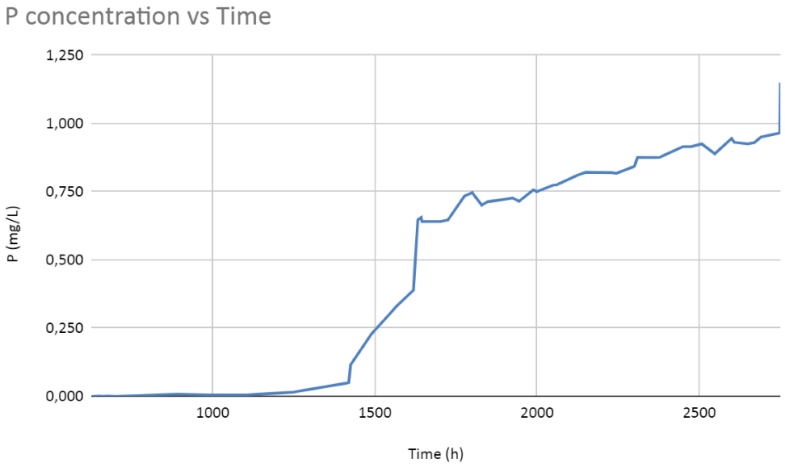

Figure 11. BTC graph which represents the effluent solution concentration (mg/L) vs the time (h).

The basaluminite adsorption capacity is calculated with the following equation: [41]

$$q_t = [(Co-Ct)\cdot V]/m \quad (12)$$

Q_t represents the time-dependent adsorption efficiency expressing as adsorbate adsorbed (mg)/adsorbent used (g). C (ppm) represents the initial (Co) (1.13 ppm P) and time-dependent (Ct) concentration of the analyte dissolved in a solution volume (V(L)) which is passed through the column with a 2.5 mL/min flow. Finally, m represents the adsorbent mass (g). With qt and the reaction time (t), a graph (Figure 12) is plotted to study the P adsorption capacity of the basaluminite.

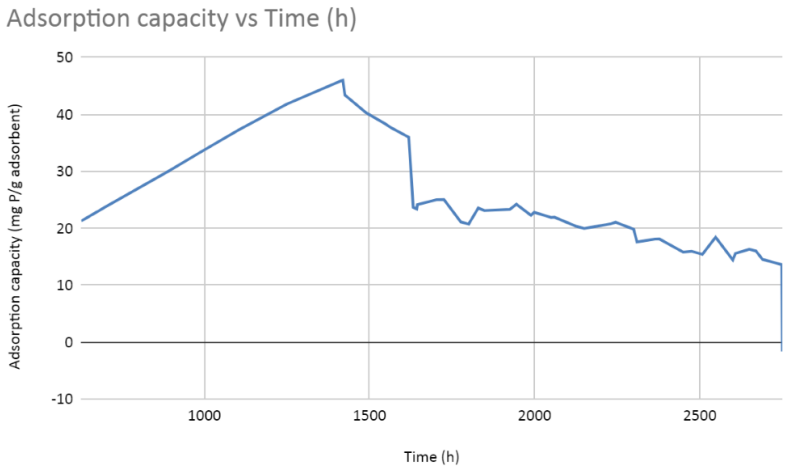

Figure 12. Representation of the basaluminite adsorption capacity (mg/g) vs the time (h).

The P adsorption capacity of the basaluminite along the time is observed in Figure 12. As time goes by, the adsorption capacity increases until it reaches the maximum adsorption capacity (q_{max}) after almost 60 days. At this point, q_{max} value is 46.0 mg P/g basaluminite. After surpassing q_{max}, the basaluminite P adsorption capacity decreases because the adsorbent starts to become saturated.

The calculated q_{max} value is comparable with that obtained in Marqués study, 40.5 mg P/g natural basaluminite, experiment carried out in a similar fixed-bed column setup and with the same P concentration inflow.[39] Thus, the value of the natural basaluminite is similar to the 46.0 mg/g raised with the synthetic salt under similar conditions. García (2017) also studied the P adsorption capacity of the synthetic basaluminite with a batch experiment raising a q_{max} value of 82.0 mg P/g synthetic basaluminite using a Langmuir isotherm model. [42] This value is higher than the obtained in this study probably because the experimental conditions, as the pH,

the solid-liquid ratio and the initial P concentration, were different in comparison that developed in this study.

Deliyanni et al. (2007) studied P sorption onto activated aluminum oxide and aluminum hydroxide gel which reached P adsorption capacities of 13.8 and 28.0 mg P/ g adsorbent, respectively.[43]. Although the adsorbents are Al salts, presents P sorption capacities lower than basaluminite, which may suggest that this residue is a promising P sorbent.

The basaluminite q_{max} can be also compared with the results presented by Sibrell et al. (2009) for P adsorption of AMD sludges (a mix of Al and Fe oxyhydroxides). The AMD sludge presented a q_{max} of 24.0 mg P/g of sorbent (with 1 ppm P solution).[32] Wei et al. (2008) were also studied the P adsorption capacity of the AMD sludge with a maximum sorption capacity of 3.0 mg P/g sorbent.[44] Thus, basaluminite has a better adsorption capacity than the AMD sludge.

Schwertmannite is a common mineral that precipitates as AMD sludge and its P sorption capacity could be also comparable with that of basaluminite. The schwertmannite capacity as P adsorbent has been studied by Arellano (2017), obtaining q_{max} values of 46.9 mg/g and 28.3 mg/g for synthetic and natural schwertmannite, respectively. In this case, there is an important difference in sorption capacity between synthetic and natural mineral. Despite this, the value of the synthetic schwertmannite is almost equal to that calculated in the present work for synthetic basaluminite. Besides, Arellano (2017) studied sorption capacity through breakthrough curve experiments. The results of these experiments with synthetic and natural schwertmannite reached 600 and 1200 bed volumes, respectively, until the exhaustion point. [45] The bed volumes, which indicates the number of times a pore volume of water passed through the column, were calculated with Equation 13 for the basaluminite column presented in this work:

$$BV=(Q\cdot t)/Vpores \quad (13)$$

Where the product between the input flow (Q) and the experiment time (t), which is the total volume of the solution that was passed through the column for this time is calculated. And then, dividing this volume by the pore volume, the number of bed volumes passed through the column is obtained as shown in Figure 13.

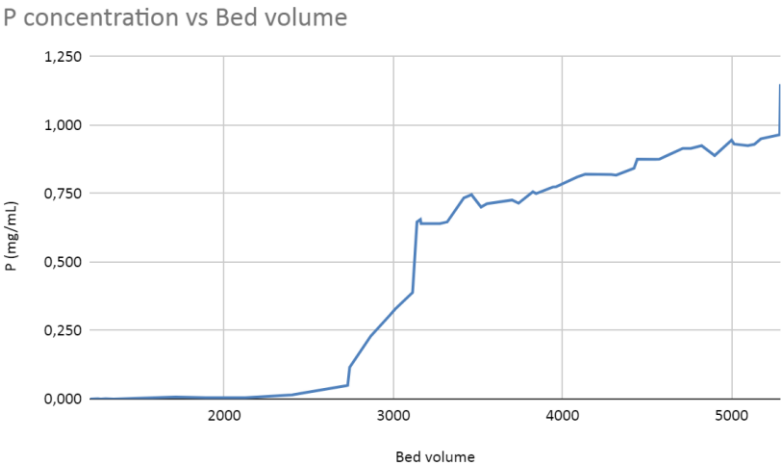

Figure 13. Representation of the P concentration (mg/L) vs the bed volume capacity of the column.

As Figure 13 shows, 4800 bed volumes had passed through the column at the exhaustion point. This value of bed volumes is higher than those calculated by Arellano (2017) for schwertmannite columns, which could indicate higher load of treatment. However, the P concentration of the input solution was different between basaluminite and schwertmannite columns, so in order to better compare its efficiency, the amount of P treated was calculated.

Table 3. Comparison of the mass balance results with the Arellano study with schwertmannite. [45]

Adsorbent type	Total treated volume (L)	Input flow (mL/min)	P concentration (mg/L)	Mass of P (g)
Synthetic basaluminite	370.40	2.50	1.13	423.07
Synthetic schwertmannite	39.17	0.80	5.00	195.84
Natural schwertmannite	66.82	0.80	5.00	334.10

As Table 3 shows, even having similar P sorption capacities, basaluminite column has been able to treat higher load of P. Thus, the Al salt column is better for the P removal than the schwertmannite column.

Literature has reported other different kind of P adsorbents. Hence, a synthesized magnetic iron oxide (MIO) studied by Choi et al. (2016) obtained a maximum sorption capacity of 15.2 mg P/g MIO.[46] Nguyen et al. (2016) used volcanic ash soil (VAS) as P adsorbent obtaining q_{max} of 2.9 mg P/g VAS for batch studies and 5.6 mg P/g VAS for column studies.[47] Shanableh et al. (2016) studied bentonite, an aluminum phyllosilicate clay. They added Fe^{3+} and Al^{3+} to improve its P adsorption capacities. The maximum sorption capacities obtained was ranged from 5.6-11.3 mg P/g sorbent.[48] Bone charcoal (BC) has also been studied as a possible sorbent of P. Concretely, Ghaneian et al. (2014) have obtained a maximum sorption capacity of 30.2 mg P/g BC.[49]

Finally, Carrero et al. (2017) also studied the As adsorption in basaluminite as adsorbent, obtaining a maximum sorption capacity of 52.7 mg As/g basaluminite.[50] Fukushi (2003) calculated an As adsorption capacity in schwertmannite of 33.5 mg/g. These results indicate that P and As have similar sorption capacities in these minerals.[51] Thus, these elements could compete for the adsorbent because they have similar chemical properties in aqueous medium.

9. CONCLUSIONS

After this project has come to its end, the main three conclusions mentioned below have been reached:

1. The column with synthetic basaluminite has 0.34 of porosity and 31.2 min of average residence time. The column with natural basaluminite has a bit bigger porosity value because the column with the synthetic adsorbent was more compact. Similarly, the column with natural basaluminite has a bigger average residence time than the column with the synthetic salt because the natural adsorbent has more pores volume.
2. Once this study has been completed, synthetic basaluminite can be considered as a remarkable P adsorbent with a maximum adsorption capacity of 46.0 mg P/g basaluminite. The results of most of the studies mentioned show lower levels of P sorption capacity at short-time than the study carried out with synthetic basaluminite. For example, the activated aluminum oxide and the aluminum hydroxide gel, two commercial reagents, or other P adsorbents such as VAS, MIO, BC among others that obtained lower P adsorption values than synthetic basaluminite. These comparisons determine that this AMD residue is one of best P adsorbents with a one of the highest P adsorption capacities.
3. The comparison of P sorption in fixed-bed columns of basaluminite and schwertmannite, indicates that both residues are remarkable adsorbents but for their experimental conditions, basaluminite column has been able to treat higher load of P, suggesting that, this AMD residue is better than the Fe salt for P adsorption.

Therefore, most of the objectives proposed at the beginning of the project have been accomplished. The good adsorption capacity of the synthetic basaluminite, as expected, has been confirmed. As a conclusion, this non-conventional material, which was a residue at first, has proved to be a remarkable P adsorbent both short-term and long-term operation. For the next studies with basaluminite, it could be interesting to study the possibility to reuse this adsorbent more than one time. Besides, the adsorption capacity of the basaluminite could be

tested in a solution with other anions such as chlorides, sulfates or nitrates, which simulates marine waters. It would have be interesting to know how effective is the adsorbent if there is a competence between phosphates and the other anions which could decrease the basaluminite adsorption capacity.

10. REFERENCES

[1] Valsami-Jones, E.; The geochemistry and mineralogy of phosphorus. In *Phosphorus in Environmental Technology: Principles and Applications*; International Water Association, 2015; Vol. 4, pp 20-37. https://doi.org/10.2166/9781780402758.

[2] Withers, P. J. A.; Bowes, M. J. Phosphorus the Pollutant. In *Phosphorus: Polluter and Resource of the Future – Removal and Recovery from Wastewater*; International Water Association, 2018; Vol. 17, pp 1–20. https://doi.org/10.2166/9781780408361.

[3] Denison, F. H.; Haygarth, P. M.; House, W. A.; Bristow, A. W. The Measurement of Dissolved Phosphorus Compounds: Evidence for Hydrolysis during Storage and Implications for Analytical Definitions in Environmental Analysis. *Int. J. Environ. Anal. Chem.* **1998**, *69* (2), 111–123. https://doi.org/10.1080/03067319808032579.

[4] D.E.C. Corbridge, *Phosphorus: An Outline of its Chemistry, Biochemistry and Technology*, Elsevier, Amsterdam, 1990, doi: 10.1002/crat.19810160411.

[5] Rashchi, F.; Finch, J. A. Polyphosphates: A Review. Their Chemistry and Application with Particular Reference to Mineral Processing. *Miner. Eng.* **2000**, *13* (10), 1019–1035. https://doi.org/10.1016/S0892-6875(00)00087-X.

[6] Valsami-Jones, E.; Preface. In *Phosphorus in Environmental Technology: Principles and Applications*; International Water Association, 2015; Vol. 4. https://doi.org/10.2166/9781780402758.

[7] Farmer, A. M.; Phosphate pollution: A global overview of the problem. In *Phosphorus: Polluter and Resource of the Future – Removal and Recovery from Wastewater*; International Water Association, 2018; Vol. 17, pp 35-44. https://doi.org/10.2166/9781780408361.

[8] Streams. *Nutrient Criteria Technical Guidance Manual: Rivers and Streams*; 2000.

[9] Ministerio de Obras Públicas, Transportes y Medio Ambiente «BOE» no. 77, published on 29 March 1996 and actualized on 12 september 2015, Reference: BOE-A-1996-7159.

[10] Directive, EU Urban Wastewater. Council Directive of 21. May 1991 concerning urban wastewater treatment (91/271/EEC), Official Journal of the European Communities, 1991.

[11] Metcalf & Eddy Inc.; Tchobanoglous, G.; Burton, F. L.; Stensel, H. D. Chapter 13: Water Reuse. In *Wastewater Engineering - Treatment and Reuse*; McGraw-Hill, 2003; pp 1345–1446.

[12] Genz, A.; Kornmüller, A.; Jekel, M. Advanced Phosphorus Removal from Membrane Filtrates by Adsorption on Activated Aluminium Oxide and Granulated Ferric Hydroxide. *Water Res.* **2004**, *38* (16), 3523–3530. https://doi.org/10.1016/j.watres.2004.06.006.

[13] Kofinas, P.; Kioussis, D. R. Reactive Phosphorus Removal from Aquaculture and Poultry Productions Systems Using Polymeric Hydrogels. *Environ. Sci. Technol.* **2003**, *37* (2), 423–427. https://doi.org/10.1021/es025950u.

[14] Zarrabi, M.; Soori, M. M.; Sepehr, M. N.; Amrane, A.; Borji, S.; Ghaffari, H. R. Removal of Phosphorus by Ion-Exchange Resins: Equilibrium, Kinetic and Thermodynamic Studies. *Environ. Eng. Manag. J.* **2014**, *13* (4), 891–903. https://doi.org/10.30638/eemj.2014.093.

[15] Liu, H.; Sun, X.; Yin, C.; Hu, C. Removal of Phosphate by Mesoporous ZrO2. *J. Hazard. Mater.* **2008**, *151* (2–3), 616–622. https://doi.org/10.1016/j.jhazmat.2007.06.033.

[16] Ruihua, L.; Lin, Z.; Tao, T.; Bo, L. Phosphorus Removal Performance of Acid Mine Drainage from Wastewater. *J. Hazard. Mater.* **2011**, *190* (1–3), 669–676. https://doi.org/10.1016/j.jhazmat.2011.03.097.

[17] Bigham, J. M.; Nordstrom, D. K. Iron and Aluminum Hydroxysulfates from Acid Sulfate Waters. *Sulfate Miner. Crystallogr. Geochemistry, Environ. Significance* **2019**, *40*, 351–403. https://doi.org/10.2138/rmg.2000.40.7.

[18] Ayora, C.; Caraballo, M. A.; Macias, F.; Rötting, T. S.; Carrera, J.; Nieto, J. M. Acid Mine Drainage in the Iberian Pyrite Belt: 2. Lessons Learned from Recent Passive Remediation Experiences. *Environ. Sci. Pollut. Res.* **2013**, *20* (11), 7837–7853. https://doi.org/10.1007/s11356-013-1479-2.

[19] Watzlaf, G. R.; Kairies, C. L.; Schroeder, K. T.; Danehy, T.; Beam *Quantitative results from the flushing of four reducing and alkalinity-producing systems 1*, West Virginia Surface Mine Drainage Task Force Symposium, 2002.

[20] Rötting, T. S.; Thomas, R. C.; Ayora, C.; Carrera, J. Passive Treatment of Acid Mine Drainage with High Metal Concentrations Using Dispersed Alkaline Substrate. *J. Environ. Qual.* **2008**, *37* (5), 1741–1751. https://doi.org/10.2134/jeq2007.0517.

[21] Nieto, J. M.; Sarmiento, A. M.; Canovas, C. R.; Olias, M.; Ayora, C. Acid Mine Drainage in the Iberian Pyrite Belt: 1. Hydrochemical Characteristics and Pollutant Load of the Tinto and Odiel Rivers. *Environ. Sci. Pollut. Res.* **2013**, *20* (11), 7509–7519. https://doi.org/10.1007/s11356-013-1634-9.

[22] Carrero, S.; Fernandez-Martinez, A.; Pérez-López, R.; Lee, D.; Aquilanti, G.; Poulain, A.; Lozano, A.; Nieto, J. M. The Nanocrystalline Structure of Basaluminite, an Aluminum Hydroxide Sulfate from Acid Mine Drainage. *Am. Mineral.* **2017**, *102* (12), 2381–2389. https://doi.org/10.2138/am-2017-6059.

[23] Kenngott, A. Mineralogische Notizen 9. Felsőbányt identisch mit Hydrargillit. *Sitzungsber. Akad. Wien* **1853**, *10*, 294.

[24] Haidinger, M. W. Über den Felsöbányt, eine neue Mineralspecies. *Sitzungsber. Akad. Wien* **1854**, *12*, 183-190.

[25] Bannister, F. A.; Hollingworth, S. E. Two New British Minerals [1]. *Nature*. Nature Publishing Group 1948, p 565. https://doi.org/10.1038/162565a0.

[26] Brydon, J.; E.-Singh, S. S. The nature of the synthetic crystalline basic aluminium sulphates as compared with basaluminite. *Canad. Mineral.* **1969**, *9*, 644-654.

[27] Clayton, F. Hydrobasaluminitc and basaluminite from Chickerell. *Dorset. Min. Mag.* **1980**, *43*, 931-937.

[28] Weiszburg; T.-Papp, G. On the relationship of basaluminite and felsőbányaite. *15th Gen Meeting IMA* **1990**, *2*, 713-715.

[29] Farkas, L.; Pertlik, F. Crystal structure determinations of Felsőbányaite and Basaluminite, $Al_4(SO_4)(OH)_{10}{\cdot}4H_2O$. *Ada Mineralogica-Petrographica, Szeged. XXXVIII.* **1997**, 5-15.

[30] Adams, F.; Rawajfih, Z. Basaluminite and Alunite: A Possible Cause of Sulfate Retention by Acid Soils1. *Soil Sci. Soc. Am. J.* **1977**, *41* (4), 686-692. https://doi.org/10.2136/sssaj1977.03615995004100040013x.

[31] Carrero, S.; Fernandez-Martinez, A.; Pérez-López, R.; Nieto, J. M. Basaluminite Structure and Its Environmental Implications. *Procedia Earth Planet. Sci.* **2017**, *17*, 237–240. https://doi.org/10.1016/j.proeps.2016.12.080.

[32] Sibrell, P. L.; Montgomery, G. A.; Ritenour, K. L.; Tucker, T. W. Removal of Phosphorus from Agricultural Wastewaters Using Adsorption Media Prepared from Acid Mine Drainage Sludge. *Water Res.* **2009**, *43* (8), 2240–2250. https://doi.org/10.1016/j.watres.2009.02.010.

[33] Bunce, J. T.; Ndam, E.; Ofiteru, I. D.; Moore, A.; Graham, D. W. A Review of Phosphorus Removal Technologies and Their Applicability to Small-Scale Domestic Wastewater Treatment Systems. *Frontiers in Environmental Science*. Frontiers Media S.A. February 22, 2018, p 8. https://doi.org/10.3389/fenvs.2018.00008.

[34] Violante, A.; Rao, M. A.; De Chiara, A.; Gianfreda, L. Sorption of Phosphate and Oxalate by a Synthetic Aluminium Hydroxysulphate Complex. *Eur. J. Soil Sci.* **1996**, *47* (2), 241–247. https://doi.org/10.1111/j.1365-2389.1996.tb01395.x.

[35] Rietra, R. P. J. J.; Hiemstra, T.; Van Riemsdijk, W. H. Sulfate Adsorption on Goethite. *J. Colloid Interface Sci.* **1999**, *218* (2), 511–521. https://doi.org/10.1006/jcis.1999.6408.

[36] Lozano, A.; Fernández-Martínez, A.; Ayora, C.; Poulain, A. Local Structure and Ageing of Basaluminite at Different PH Values and Sulphate Concentrations. *Chem. Geol.* **2018**, *496* (July), 25–33. https://doi.org/10.1016/j.chemgeo.2018.08.002.

[37] Sperlich, A.; Werner, A.; Genz, A.; Amy, G.; Worch, E.; Jekel, M. Breakthrough Behavior of Granular Ferric Hydroxide (GFH) Fixed-Bed Adsorption Filters: Modeling and Experimental Approaches. *Water Res.* **2005**, *39* (6), 1190–1198. https://doi.org/10.1016/j.watres.2004.12.032.

[38] Murphy, J.; Riley, J. P. A Modified Single Solution Method for the Determination of Phosphate in Natural Waters. *Anal. Chim. Acta* **1962**, *27* (C), 31–36. https://doi.org/10.1016/S0003-2670(00)88444-5.

[39] Marqués Pons, J. Phosphorus removal using fixed-bed column of natural basaluminite, TFG Grau en Química, 2020, Universitat de Barcelona, pp 34-40.

[40] Levenspiel, O.; Costa López, J. Flujo de Fluídos e Intercabio de Calor; Reverté, 1998.

[41] Li, Z.; Kang, W.; Wei, N.; Qiu, J.; Sun, C.; Cheng, B. Preparation of a Polyvinylidene Fluoride Tree-like Nanofiber Mat Loaded with Manganese Dioxide for Highly Efficient Lead Adsorption. *RSC Adv.* **2017**, *7* (14), 8220–8229. https://doi.org/10.1039/c6ra27865e.

[42] García Cardona, J. Removal of phosphorus from sewage using basaluminite, a residue from acid mine drainage treatment. TFG Grau en Química, 2017, Universitat de Barcelona, pp. 23-24

[43] Deliyanni, E. A.; Peleka, E. N.; Lazaridis, N. K. Comparative Study of Phosphates Removal from Aqueous Solutions by Nanocrystalline Akaganéite and Hybrid Surfactant-Akaganéite. *Sep. Purif. Technol.* **2007**, 52 (3), 478–486. https://doi.org/10.1016/j.seppur.2006.05.028.

[44] Wei, X.; Viadero, R.C.; Bhojappa, S. Phosphorus removal by acid mine drainage sludge from secondary effluents of municipal wastewater treatment plants. *Water research*. **2008**, 42, 3275-3284. https://doi.org/10.1016/j.watres.2008.04.005

[45] Arellano Valenzuela, A. Retención de fósforo mediante residuos de tratamientos de aguas ácidas de mina. TFM Màster en Enginyeria Química, 2017, Universitat Politècnica de Catalunya, pp. 97.

[46] Choi, J.; Chung, J.; Lee, W.; Kim, J.O. Phosphorous adsorption on synthesized magnetite in wastewater. *Journal of Industrial and Engineering Chemistry*. **2016**, 34, 198–203. https://doi.org/10.1016/j.jiec.2015.11.008

[47] Nguyen, HV.; Maeda, M. Removal of phosphorus from water by using volcanic ash soil (VAS): batch and column experiments. *Water science and technology*. **2016**, 74, 6, 1326-1334. https://doi.org/10.2166/wst.2016.297

[48] Shanableh, A.; Enshasi, G.; Elsergany, M. Phosphorous adsorption using Al^{3+}/Fe^{3+} modified bentonite adsorbents-effect of Al^{3+}/Fe^{3+} combinations. *Desalination and water treatment*. **2016,** 57, 33, 15628-15634. https://doi.org/10.1080/19443994.2015.1129510

[49] Ghaneian, M. T.; Ghanizadeh, G.; Alizadeh, M. T. H.; Ehrampoush, M. H.; Said, F. M. Equilibrium and Kinetics of Phosphorous Adsorption onto Bone Charcoal from Aqueous Solution. *Environ. Technol. (United Kingdom)* **2014**, 35 (7), 882–890. https://doi.org/10.1080/09593330.2013.854838.

[50] Carrero, S.; Fernandez-Martinez, A.; Pérez-López, R.; Poulain, A.; Salas-Colera, E.; Nieto, J. M. Arsenate and Selenate Scavenging by Basaluminite: Insights into the Reactivity of Aluminum Phases in Acid Mine Drainage. *Environ. Sci. Technol.* **2017**, 51 (1), 28–37. https://doi.org/10.1021/acs.est.6b03315.

[51] Fukushi, K.; Sato, T.; Yanase, N. Solid-Solution Reactions in As(V) Sorption by Schwertmannite. *Environ. Sci. Technol.* **2003**, *37* (16), 3581–3586. https://doi.org/10.1021/es026427i.

.

11. ACRONYMS

P: Phosphorus

BOE: Spanish Official State Gazette

PAO: Phosphorus Accumulator's Organisms

PHB: Polyhydroxybutyrate

AMD: Acid Mine Drainage

ALD: Anoxic Limestone Drain

RAPS: Reducing and Alkalinity-Producing Systems

DAS: Disperse Alkaline Substrate

IPB: Iberian Pyrite Belt

XRD: X-Ray Powder Diffraction

IMA: International Mineralogy Association

BTC: Breakthrough curve

SRP: Soluble Reactive Phosphorus

MRP: Molybdate Reactive Phosphorus

DRP: Dissolved Reactive Phosphorus

V: Volume

P: Column porosity

Q: Input flow

t: Mean time

C/C_o: Relative conductivity

A: Column area

h: Column height

r: Column radio

R_t: Average residence time

q_t: Time-dependent adsorption efficiency

C_o: Initial concentration

C_t: Time-dependent concentration

m: Adsorbent mass

q_{max}: Maximum adsorption capacity

B: Bed volume

MIO: Magnetic Iron Oxide

VAS: Volcanic Ash Soil

BC: Bone Charcoal

APPENDICES

APPENDIX 1: RESULTS DATA TABLES

Table 4: Relevant data to plot the decline curve of the tracer test.

Time(min)	Relative conductivity
18:04:00	1
18:05:00	1
18:06:00	0,9980582524
18:07:00	0,9980582524
18:08:00	0,9980582524
18:09:00	0,9980582524
18:10:00	0,9961165049
18:11:00	0,9961165049
18:12:00	0,9961165049
18:13:00	0,9941747573
18:14:00	0,9941747573
18:15:00	0,9941747573
18:16:00	0,9941747573
18:17:00	0,9941747573
18:18:00	0,9941747573
18:19:00	0,9922330097
18:20:00	0,9941747573
18:21:00	0,9922330097
18:22:00	0,9922330097
18:23:00	0,9922330097
18:24:00	0,9922330097
18:25:00	0,9922330097
18:26:00	0,9922330097
18:27:00	0,9922330097
18:28:00	0,9922330097
18:29:00	0,9922330097
18:30:00	0,9922330097
18:31:00	0,9922330097
18:32:00	0,9922330097
18:33:00	0,9922330097
18:34:00	0,9941747573
18:35:00	0,9941747573

18:36:00	0,9941747573
18:37:00	0,9922330097
18:38:00	0,9941747573
18:39:00	0,9941747573
18:40:00	0,9922330097
18:41:00	0,9941747573
18:42:00	0,9922330097
18:43:00	0,9941747573
18:44:00	0,9922330097
18:45:00	0,9922330097
18:46:00	0,9922330097
18:47:00	0,9922330097
18:48:00	0,9902912621
18:49:00	0,9902912621
18:50:00	0,9902912621
18:51:00	0,9902912621
18:52:00	0,9902912621
18:53:00	0,9883495146
18:54:00	0,9883495146
18:55:00	0,9883495146
18:56:00	0,9883495146
18:57:00	0,9883495146
18:58:00	0,9883495146
18:59:00	0,9883495146
19:00:00	0,9883495146
19:01:00	0,986407767
19:02:00	0,9883495146
19:03:00	0,986407767
19:04:00	0,986407767
19:05:00	0,9883495146
19:06:00	0,986407767
19:07:00	0,986407767
19:08:00	0,986407767
19:09:00	0,986407767
19:10:00	0,986407767
19:11:00	0,9883495146
19:12:00	0,9883495146
19:13:00	0,986407767
19:14:00	0,9883495146
19:15:00	0,986407767
19:16:00	0,986407767
19:20:00	0,986407767

19:21:00	0,9825242718
19:22:00	0,9825242718
19:23:00	0,9786407767
19:24:00	0,9766990291
19:25:00	0,9747572816
19:26:00	0,9708737864
19:27:00	0,9650485437
19:28:00	0,959223301
19:29:00	0,9514563107
19:30:00	0,9436893204
19:31:00	0,9359223301
19:32:00	0,9281553398
19:33:00	0,9203883495
19:34:00	0,9106796117
19:35:00	0,9009708738
19:36:00	0,8912621359
19:37:00	0,8834951456
19:38:00	0,8757281553
19:39:00	0,867961165
19:40:00	0,8621359223
19:41:00	0,8563106796
19:42:00	0,8466019417
19:43:00	0,8368932039
19:44:00	0,8252427184
19:45:00	0,8155339806
19:46:00	0,8058252427
19:47:00	0,7980582524
19:48:00	0,7922330097
19:49:00	0,7883495146
19:50:00	0,786407767
19:51:00	0,7805825243
19:52:00	0,7747572816
19:53:00	0,7689320388
19:54:00	0,7611650485
19:55:00	0,7553398058
19:56:00	0,7475728155
19:57:00	0,7378640777
19:58:00	0,732038835
19:59:00	0,7145631068
20:00:00	0,6932038835
20:01:00	0,6776699029
20:02:00	0,6660194175

20:03:00	0,6524271845
20:04:00	0,6446601942
20:05:00	0,6330097087
20:06:00	0,6213592233
20:07:00	0,6116504854
20:08:00	0,6019417476
20:09:00	0,5922330097
20:10:00	0,5825242718
20:11:00	0,572815534
20:12:00	0,5611650485
20:13:00	0,5514563107
20:14:00	0,5398058252
20:15:00	0,5300970874
20:16:00	0,5203883495
20:17:00	0,5106796117
20:18:00	0,5029126214
20:19:00	0,4951456311
20:20:00	0,4854368932
20:21:00	0,4796116505
20:22:00	0,4737864078
20:23:00	0,467961165
20:24:00	0,4601941748
20:25:00	0,4524271845
20:26:00	0,4446601942
20:27:00	0,4368932039
20:28:00	0,4291262136
20:29:00	0,4233009709
20:30:00	0,4213592233
20:31:00	0,4058252427
20:32:00	0,3961165049
20:33:00	0,3902912621
20:34:00	0,3844660194
20:35:00	0,3805825243
20:36:00	0,3747572816
20:37:00	0,3650485437
20:38:00	0,3572815534
20:39:00	0,3436893204
20:40:00	0,332038835
20:41:00	0,3281553398
20:42:00	0,3165048544
20:43:00	0,3067961165
20:44:00	0,3009708738

20:45:00	0,2951456311
20:46:00	0,2854368932
20:47:00	0,2776699029
20:48:00	0,2699029126
20:49:00	0,2640776699
20:50:00	0,2601941748
20:51:00	0,2601941748
20:52:00	0,2504854369
20:53:00	0,2427184466
20:54:00	0,240776699
20:55:00	0,2349514563
20:56:00	0,227184466
20:57:00	0,2252427184
20:58:00	0,2194174757
20:59:00	0,2155339806
21:00:00	0,2116504854
21:01:00	0,2116504854
21:02:00	0,2077669903
21:03:00	0,2077669903
21:04:00	0,2038834951
21:05:00	0,2
21:06:00	0,2
21:07:00	0,1980582524
21:08:00	0,1980582524
21:09:00	0,1961165049
21:10:00	0,1961165049
21:11:00	0,1941747573
21:12:00	0,1922330097
21:13:00	0,1902912621
21:14:00	0,1883495146
21:15:00	0,186407767
21:16:00	0,1825242718
21:17:00	0,1805825243
21:18:00	0,1747572816
21:19:00	0,1689320388
21:20:00	0,1631067961
21:21:00	0,1631067961
21:22:00	0,159223301
21:23:00	0,1533980583
21:24:00	0,1495145631
21:25:00	0,1436893204
21:26:00	0,1378640777

21:27:00	0,1339805825
21:28:00	0,132038835
21:29:00	0,1281553398
21:30:00	0,1262135922
21:31:00	0,1242718447
21:32:00	0,1223300971
21:33:00	0,1203883495
21:34:00	0,1184466019
21:35:00	0,1184466019
21:36:00	0,1165048544
21:37:00	0,1145631068
21:38:00	0,1126213592
21:39:00	0,1106796117
21:40:00	0,1106796117
21:41:00	0,1087378641
21:42:00	0,1087378641
21:43:00	0,1087378641
21:44:00	0,1087378641
21:45:00	0,1106796117
21:46:00	0,1106796117
21:47:00	0,1106796117
21:48:00	0,1126213592
21:49:00	0,1145631068
21:50:00	0,1145631068
21:51:00	0,1145631068
21:52:00	0,1145631068
21:53:00	0,1145631068
21:54:00	0,1145631068
21:55:00	0,1126213592
21:56:00	0,1126213592
21:57:00	0,1126213592
21:58:00	0,1126213592
21:59:00	0,1106796117
22:00:00	0,1087378641
22:01:00	0,1067961165
22:02:00	0,1029126214
22:03:00	0,1009708738
22:04:00	0,09708737864
22:05:00	0,09514563107
22:06:00	0,0932038835
22:07:00	0,09126213592
22:08:00	0,08932038835

22:09:00	0,08932038835
22:10:00	0,08737864078
22:11:00	0,0854368932
22:12:00	0,0854368932
22:13:00	0,08349514563
22:14:00	0,08349514563
22:15:00	0,08155339806
22:16:00	0,08155339806
22:17:00	0,07961165049

Table 5: Data for the breakthrough curve experiment.

Time (h)	P (mg/L)
627,5	0,000
651,5	0,001
659,5	0,000
675,5	0,001
699,5	0,000
890,6	0,008
983,1	0,005
1104,6	0,005
1248,6	0,015
1272,6	0,020
1414,47	0,048
1419,6	0,050
1425,6	0,115
1490,1	0,229
1548,6	0,305
1565,1	0,328
1619,1	0,389
1632,6	0,647
1643,1	0,656
1645,25	0,640
1703,1	0,640
1725,6	0,647
1776,6	0,734
1800,6	0,746
1802,1	0,743
1829,6	0,701
1847,75	0,713
1925	0,727

1945	0,715
1989	0,757
1999	0,750
2050	0,774
2060	0,775
2125	0,811
2150	0,821
2230	0,820
2245	0,818
2300	0,843
2310	0,876
2365	0,875
2378	0,876
2398	0,887
2450	0,915
2475	0,915
2508	0,925
2548	0,889
2600	0,945
2608	0,931
2650	0,925
2670	0,930
2690	0,950
2748	0,965
2750	1,150

APPENDIX 2: PROCEDURE OF THE PREPARATION OF BASALUMINITE AND ALUMINUM OXIDE COLUMNS

Hence, 5 g of the salts were weighed on an analytical balance. 5.0116 g of aluminum oxide and 5.6444 of basaluminite were weighed. Then, the salts were mixed in two beakers with the pine chips previously sieved for giving the same chip size and washed to eliminate some organic matter. In the baker which had the basaluminite, the mixture weighed 146.21 g. In the other, the mixture with aluminum oxide and pine weighed 130.00 g. Approximately, in both bakers, there was a 1:6 grams ratio between the aluminum salts and the wood.

Firstly, two centimeters of silica pearls were added in both columns. Secondly, the mixture of aluminum oxide and wood was added to the blue marked column and the other to the yellow marked column, bit by bit. Hence, when the mixture was added, it could be compacted with pressure. The mixtures were added completely to their respective columns. The basaluminite column had 12 centimeters of the mixture and the aluminum oxide column had 11 cm. Finally, one centimeter of silica pearls was included in both columns another time.

Then, the solution of phosphates was prepared. The objective was to prepare a solution which simulates wastewater. First, the following salts were weighed with an analytical balance: 0.2224 g of KH_2PO_4 (for 10 ppm P), 0.7746 g of $NaHCO_3$ (for 155 ppm), 0.1421 g of $MgCl_2 \cdot 6H_2O$ (for 25 ppm), 0.2146 g of $CaCl_2 \cdot 2H_2O$ (for 37 ppm). Then, these salts were added with MilliQ® ultrapure water into a 5 L flask. The solution pH measured with the Thermo-scientific Orion Dual Star pH-meter was 7.227.

Once the 10 ppm phosphorus solution passed through the column, using the three-way valve solutions sample was recollected. Only 2 samples of each column were collected. The same day in which the solution was added to the column, the pH of basaluminite column was 4.171 and the pH of the Al oxide column was 4.667. The following day the pH was 4.315 and 6.684 respectively.

On the first day, the pH solution decreased in two cases when it passes through the column. On the second day, the pH solution increases in both columns. Specifically, basaluminite has a lower impact on the solution pH than the Al oxide. However, these results are not significant because there are only two samples.